

2015-09-18

# Combined uncertainty estimation for the determination of the dissolved iron amount content in seawater using flow injection with chemiluminescence detection

Floor, GH

<http://hdl.handle.net/10026.1/5315>

---

10.1002/lom3.10057

LIMNOLOGY AND OCEANOGRAPHY-METHODS

Wiley

---

*All content in PEARL is protected by copyright law. Author manuscripts are made available in accordance with publisher policies. Please cite only the published version using the details provided on the item record or document. In the absence of an open licence (e.g. Creative Commons), permissions for further reuse of content should be sought from the publisher or author.*

1 Disclaimer: This is a pre-publication version. Readers are recommended to consult the  
2 full published version for accuracy and citation. Published in Limnology and  
3 Oceanography: Methods, 13, 673–686 (2015), doi: 10.1002/lom3.10057.  
4

5 **Combined uncertainty estimation for the determination of the dissolved iron**  
6 **amount content in seawater using flow injection with chemiluminescence**  
7 **detection.**

8

9 G. H. Floor<sup>1a</sup>, R. Clough<sup>2</sup>, M. C. Lohan<sup>2</sup>, S. J. Ussher<sup>2</sup>, P. J. Worsfold<sup>2</sup>, C. R. Quétel<sup>1\*</sup>.

10 1. Institute for Reference Materials and Measurements, Joint Research Centre–European Commission,  
11 111 Retieseweg, 2440 Geel, Belgium.

12 2. Biogeochemistry Research Centre, School of Geography, Earth and Environmental Sciences, Plymouth  
13 University, Plymouth, PL4 8AA, United Kingdom

14 a: Currently at GFZ German Research Centre for Geosciences, Helmholtz Centre Potsdam,  
15 Telegrafenberg, 14473 Potsdam, Germany

16 \* Corresponding author: [Christophe.Quetel@ec.europa.eu](mailto:Christophe.Quetel@ec.europa.eu)

17 **Acknowledgements**

18 This work was financially supported by the EMRP via JRP-ENV05 (Metrology for ocean salinity and acidity,  
19 GF) and JRP-ENV05-REG1 (RC). The EMRP is jointly funded by the EMRP participating countries within  
20 EURAMET and the European Union. ML was supported by a Natural Environment Research Council  
21 (NERC) grant NE/H004475/1. SU was supported by a Marie Curie Career Integration Grant (PCIG-GA-  
22 2012-333143 DISCOSAT) from the European Commission. GF acknowledges J. Snell and T. Linsinger for  
23 fruitful discussions.

24

25    **Abstract**

26    This work assesses the components contributing to the combined uncertainty budget associated with the  
27    measurement of the Fe amount content by flow injection chemiluminescence (FI-CL) in <0.2 µm filtered  
28    and acidified seawater samples. Amounts of loaded standard solutions and samples were determined  
29    gravimetrically by differential weighing. Up to 5% variations in the loaded masses were observed during  
30    measurements, in contradiction to the usual assumptions made when operating under constant loading  
31    time conditions. Hence signal intensities (V) were normalised to the loaded mass and plots of average  
32    normalized intensities (in V kg<sup>-1</sup>) versus values of the Fe amount content (in nmol kg<sup>-1</sup>) added to a 'low  
33    level' iron seawater matrix were used to produce the calibration graphs. The measurement procedure  
34    implemented and the uncertainty estimation process developed were validated from the agreement  
35    obtained with consensus values for three SAFe and GEOTRACES reference materials (D2, GS and GD).  
36    Relative expanded uncertainties for peak height and peak area based results were estimated to be  
37    around 12% and 10% (k=2) respectively. The most important contributory factors were the uncertainty  
38    on the sensitivity coefficient (i.e. calibration slope) and within-sequence-stability (i.e. the signal stability  
39    measured over several hours of operation; in this case 32 h). Therefore, an uncertainty estimation based  
40    on the intensity repeatability alone, as is often done in FI-CL studies, is not a realistic estimation of the  
41    overall uncertainty of the procedure.

42

43

44 **Introduction**

45 The ocean acts as both a sink and a source for carbon dioxide and plays an important role in regulating  
46 the global climate system (Boyd and Elwood, 2010). The dynamics of the ocean and its interaction with  
47 the atmosphere are strongly linked to the properties of seawater. Elements such as Fe limit marine  
48 primary production in approximately one third of the world's oceans (Ussher et al., 2013) and thus may  
49 have a profound effect on plankton communities and the global carbon cycle (Martin and Fitzwater, 1988;  
50 Mills et al., 2004). More reliable determinations of micronutrient elements in marine waters are thus  
51 essential to enhance our understanding of their impact on ocean productivity and processes (e.g. ocean  
52 acidification). Therefore, robust and fully validated measurement procedures are necessary, accompanied  
53 by an estimation of the overall uncertainty budget.

54 The international standard ISO/IEC 17025 (2005) states that the performance of a measurement  
55 procedure should be evaluated based on one or a combination of the following approaches: a) the use of  
56 reference materials, b) the comparison of results achieved with other methods, c) inter-laboratory  
57 comparison, d) systematic assessments of the factors influencing the result and e) the assessment of the  
58 uncertainty of the results. The Fe content of commercially available certified reference materials is at  
59 least one order of magnitude higher than most open ocean waters and are thus of limited use for  
60 method development. Therefore, test materials from inter-laboratory comparison exercises are often used  
61 instead, e.g. those collected as part of the IRONAGES, SAFe and GEOTRACES studies. However, Bowie et  
62 al. (2006) observed that discrepancies between results obtained in different laboratories during the  
63 IRONAGES comparison remained too large (e.g. up to 59% variability when using the same procedure)  
64 and differed significantly at the 95 % confidence level. Factors thought to explain these results included:  
65 (1) variations in the efficiency of the extraction of iron from the matrix during pre-concentration  
66 (resulting in different procedures measuring different fractions of iron), (2) errors in the quantification of  
67 the analytical blank, (3) inaccuracies in the system calibration and (4) underestimation of the stated  
68 uncertainty (Bowie et al, 2003; Petrov et al. 2007). Hence iron data from these exercises for the same  
69 water mass were distinctly inconsistent. Points (1) and (2) have been addressed by the SAFe (Johnson et  
70 al., 2007) and GEOTRACES (GEOTRACES, 2013) exercises but not points (3) and (4). It is thus useful to  
71 revisit these two factors and determine how realistic uncertainties can be estimated for the most  
72 commonly applied measurement procedures (particularly shipboard procedures) (see also Ussher et al.,  
73 2010b). In this respect flow injection with chemiluminescence detection (FI-CL) was chosen for this study  
74 as it is a technique that allows high temporal and spatial resolution measurements at sea without the  
75 need for sample storage and transport.

76 According to the international nomenclature, the measurement uncertainty is a "*non-negative parameter*  
77 *characterizing the dispersion of the quantity values being attributed to a measurand, based on the*  
78 *information used*" (JCGM 200, 2008). The basic purpose of an uncertainty statement is to propose a  
Geerke L&O methods 2016 PEARL

79 range of possible ‘true’ values. There are various ways of estimating uncertainties. For instance,  
80 combined uncertainty estimates can be based on data obtained by inter-laboratory or intra-laboratory  
81 studies (see e.g. Analytical Methods Committee, 1995; Nordic Committee on Food Analysis, 1997). The  
82 uncertainty estimation proposed in the Guide for Uncertainty in Measurements (GUM) is based on  
83 combining the contributions of all known sources of uncertainty (JCGM 100, 2008). In this approach, the  
84 measurement procedure is described by a mathematical model and the values and associated standard  
85 uncertainties of the different components (the input quantities) in the model must be established. The  
86 model and input data are then used to calculate the measurement result including its associated  
87 combined uncertainty.

88 The aim of this work was to study the application of the ‘GUM approach’ to the FI-CL measurement  
89 procedure. The specific objectives were to; (1) propose a set of mathematical equations (a model)  
90 describing this measurement process and allowing the estimation of a measurement uncertainty, (2)  
91 discuss the best way to assess the uncertainties of the different components in the model, (3) apply this  
92 uncertainty model to present the measurement results with their estimated combined uncertainties  
93 obtained for seawater samples from the SAFe and GEOTRACES campaigns (Lohan et al., 2006; Johnson  
94 et al., 2007) and, from the above, (4) propose a simplified equation to estimate the measurement  
95 uncertainty.

96

## 97 **Materials and procedures**

### 98 ***Reagents, materials and samples***

99 Concentrated hydrochloric acid (HCl), ammonia ( $\text{NH}_3$ , 20 – 22%) and glacial acetic acid ( $\text{CH}_3\text{CO}_2\text{H}$ ), all  
100 SpA grade, were purchased from Romil (Cambridge, UK). Hydrogen peroxide, Merck Suprapur grade was  
101 obtained from VWR (Lutterworth UK). Luminol (5-amino-2,3-dihydro-1,4-phthalazinedione), sodium  
102 carbonate and triethylenetetramine (TETA) were purchased from Sigma Aldrich (Gillingham, Dorset, UK).  
103 All high purity water (HPW),  $18.2 \text{ M}\Omega\cdot\text{cm}$ , was drawn from an ElgaStat Maxima system (Marlow, UK). All  
104 weighing was performed using an analytical balance (OH1602/C, Ohaus, Thetford, UK). The accuracy of  
105 the balance was checked daily before use using F1 Class certified weights (KERN, Albstadt, Germany). All  
106 facilities were managed under ISO 9001:2008 certification.

107 To ensure low blank Fe amount content all sample and reagent handling was undertaken in an ISO  
108 14644-1 Class 5 laminar flow hood (Bassaire, Southampton, UK) situated within an ISO 14644-1 Class 5  
109 clean room. Reagent and sample containers were made of low density polyethylene (LDPE; Nalgene,  
110 Fisher Scientific, UK) and were cleaned using established cleaning protocols for trace metals. Containers  
111 were immersed in  $\sim 1.1 \text{ M}$  trace metal grade HCl (Fisher Scientific) for at least seven days. Subsequently,

112 the containers were rinsed in copious amounts of HPW, filled with 0.01 M HCl and stored in double re-  
113 sealable plastic bags until use.

114 The main characteristics of the seawater samples used for this project are described in Table 1. Briefly,  
115 all samples were filtered at sea and then acidified either at sea or at Plymouth University (PU). Seawater  
116 samples, referred to as SWA, SWB, and SWC, containing  $\leq 0.5 \text{ nmol kg}^{-1}$  Fe were selected to prepare  
117 three different sets of calibration standards, by addition of controlled amounts of iron from a CPI  
118 International (Amsterdam, Netherlands) ICP-MS standard containing  $0.17 \text{ mol kg}^{-1}$  Fe. Experiments in this  
119 work were carried out with 0.5 L reference samples from large volumes of homogenised, bulk seawater  
120 samples (SAFe D2 and GEOTRACES GS and GD consensus mean reference materials). More details  
121 regarding the sampling, pre-treatment and bottling procedures for these materials can be found  
122 elsewhere (Jonhson et al., 2007; GEOTRACES 2013).

123

124 ***The FI-CL based measurement procedure***

125 Figure 1 describes the FI-CL manifold used for these experiments. It consists of three peristaltic pumps  
126 (Minipuls 3, Gilson, Luton, UK), one PTFE manually operated three port valve (Valve 1; Omnifit), one  
127 three port solenoid valve (Valve 2), one two-way six port electronically actuated valve (Valve 3; VICI,  
128 Valco Instruments, Schenkon, Switzerland), a thermostatic water bath (Gran, Cambridge, UK) and a  
129 photomultiplier tube (PMT; Hamamatsu H 6240-01, Hamamatsu Photonics, Welwyn Garden City, UK)  
130 containing a coiled, transparent PVC flow cell (volume 40  $\mu\text{L}$ ). The peristaltic pump tubing used was two  
131 stop accu-rated™ PVC (Elkay, Basingstoke, UK) and all other manifold tubing was 0.8 mm i.d. PTFE. The  
132 system used two poly(methyl methacrylate) columns (1 cm long, 1.5 mm i.d., volume 70  $\mu\text{L}$ ), loaded with  
133 Toyopearl AF Chelate 650 resin (Tosoh Bioscience, Stuttgart, Germany) retained with HDPE frits (BioVion  
134 F, 0.75 mm thick, 22-57  $\mu\text{m}$  pore size), to clean up the buffer and column rinse solutions. The analytical  
135 column, also loaded with Toyopearl AF Chelate 650 resin, was made of polyethylene with LDPE frits with  
136 an internal volume of 200  $\mu\text{L}$  (Global FIA, Fox Island, USA).

137 Peristaltic pump and valve control and data acquisition were performed using custom built hardware and  
138 software (Rutherford Instruments, Bodmin, UK) run under Labview v 7.1 (National Instruments, Newbury,  
139 UK). The measurement procedure, based on Obata et al. (1993), was as follows. A working solution of  
140 approximately  $0.35 \mu\text{mol kg}^{-1}$  Fe was prepared gravimetrically by serial dilution of the CPI International  
141 stock solution. This working solution was then used to gravimetrically prepare calibration standards and  
142 achieve added levels ranging from 0.15 to  $0.9 \text{ nmol kg}^{-1}$  Fe in  $0.15 \text{ nmol kg}^{-1}$  increments. All calibration  
143 standards were prepared at least 12 h before use to allow for complete equilibration of the added Fe with  
144 that present in the calibration seawater. A 20  $\mu\text{L}$  aliquot of a 10 mM  $\text{H}_2\text{O}_2$  solution was added to all  
145 calibration standards at least 2 h before use, to ensure that all Fe present was as Fe(III) (Lohan et al.,  
146 2006). The following solutions were also prepared at least 12 h before use. A 48 mM stock solution of

luminol was obtained by dissolving 0.177 g of luminol and 0.25 g of Na<sub>2</sub>CO<sub>3</sub> in 20 mL of HPW. This stock was then diluted to give a 0.24 mM working solution. The post column reagents for the chemiluminescence reaction was a mixture of 0.23 M HCl, 0.44 M NH<sub>3</sub>, 0.24 mM luminol / 0.46 mM TETA and 0.31 M H<sub>2</sub>O<sub>2</sub>. The acidified reference samples and standards of seawater were buffered to pH 3.5 with 0.35 M CH<sub>3</sub>CO<sub>2</sub>H and 0.11 M NH<sub>3</sub>. To precondition and wash the column, 0.011 M HCl was used.

To operate the FI-CL instrument, the LabVIEW software was opened and the baseline signal from the PMT monitored to check for stability. The pump controlling the eluent and post-column reagents was then activated and the baseline chemiluminescence signal recorded after the signal had stabilised. Each analytical session started with the measurement of a procedural blank (by application of the "closed sample valve" method). For this, the sample flow was stopped, by closing one port on valve 1, so that only the wash solution and ammonium acetate buffer passed over the column. The FI-CL system was then operated by loading and injecting SWA for at least 30 min to monitor stability. Subsequently, calibration seawater standards and samples were analysed. The FI-Cl manifold was fully automated and one replicate measurement consisted of the following analytical cycle. The column was conditioned for 10 s with 0.011 M HCl. Then the sample and buffer were loaded simultaneously for 60 s. The column was washed with 0.011 M HCl for 20 s. The Fe was then eluted with 0.23 M HCl for 120 s. The mass of loaded sample or standard solution was gravimetrically determined for each replicate by differential weighing. Between each sample the sample flow path was washed with HPW for 30 s followed by uptake of the fresh sample for 180 s. After each analytical session all fluid paths were flushed with 0.01 M HCl for 10 min and then with HPW for 15 min and HPW was left in the lines.

167

### 168 **Data treatment**

169 Data integration was also performed with the custom build software run in LabVIEW. The baseline, and  
170 the start and end points of the peak were set manually for each transient signal. The main calculations in  
171 this study were carried out on the basis of peak height data, as this is the commonly used practice for FI-  
172 CL measurements in the oceanographic community (and the wider FI community). Peak area  
173 measurements were also made and some of the differences observed when using peak areas are  
174 discussed below. Further data treatment, including calculations for the estimation of standard  
175 uncertainties, was carried out in Excel®. The combined uncertainties were obtained by propagating  
176 together individual uncertainty components according to the GUM (JCGM 100, 2008). In practice, a  
177 dedicated software program was used (Metrodata GmbH, 2003). The reported combined uncertainties  
178 are expanded uncertainties and reported as  $U = k u_c$  where  $u_c$  is the combined standard uncertainty and  $k$   
179 is a coverage factor equal to 2. If "*the probability distribution characterized by  $y$  and  $u_c(y)$  is  
180 approximately normal and the effective degrees of freedom of  $u_c(y)$  is of significant size*" ("greater than

181    10"), "taking  $k=2$  produces an interval having a level of confidence of approximately 95 %" (JCGM 100,  
182    2008).

183

184    **Assessment**

185    ***Definition of the measurand***

186    The GUM states that a measurement begins with an appropriate specification of the measurand, the  
187    particular quantity intended to be measured (JCGM 100, 2008). Iron exists in different physico-chemical  
188    forms in seawater. Traditionally, filtration is performed to differentiate between the different physical size  
189    fractions (Ussher et al., 2004, 2010a, Wu et al., 2001). Additionally, iron occurs in two oxidation states;  
190    Fe(II) and Fe(III). Generally, Fe(III) predominates in oxygenated waters, of which most (80–99%) is  
191    strongly complexed by organic ligands (Achterberg et al., 2001; Mawji et all, 2008; Gledhill and Buck,  
192    2012). In this study the measurand is the amount content of Fe present in <0.2 µm filtered and acidified  
193    samples and is regarded as the dissolved fraction of the Fe present in the seawaters. The aim was to  
194    obtain the Fe amount content in specific samples and therefore the uncertainties associated with the  
195    sampling process and/or the sample conditioning phase have not been considered.

196

197    ***Experimental design***

198    Three different types of experiment were performed. Firstly, the stability of the analytical procedure was  
199    checked with 5 measurements (6 replicates of each) performed over a period of 32 h for SWC (with and  
200    without H<sub>2</sub>O<sub>2</sub> addition) and a procedural blank (this was termed the "stability experiment"). Secondly, the  
201    effect of small variations in the matrix was investigated by comparing the sensitivity achieved for the  
202    three different seawaters (Table 1). On the first day, SWA was compared with SWB while on the second  
203    day SWA was compared with SWC ("matrix experiment"). Thirdly, the FI-CL based procedure was applied  
204    to the determination of iron in samples of three filtered and acidified seawater reference materials using  
205    SWA for calibration ("sample experiment").

206

207    ***Calculating the dissolved Fe amount content in the samples and mathematical description of  
208    the measurement procedure***

209    Implicit in the GUM "*is the assumption that a measurement can be modelled mathematically to the  
210    degree imposed by the required accuracy of the measurement*" (JCGM 100, 2008). A measurand Y is  
211    determined from various input quantities X<sub>i</sub> through a functional relationship. These input quantities "*may  
212    themselves be viewed as measurands and may themselves depend on other quantities, including  
213    corrections and correction factors*" "*that can contribute a significant component of uncertainty to the  
214    result of the measurement*" (JCGM 100, 2008). A mathematical description of the FI-CL measurement  
215    procedure is given through equations 1 to 5 described in Table 2. The main equation in this procedure is

216 the calculation of the dissolved Fe amount content in a sample by dividing the blank corrected sample  
217 intensity by the sensitivity of the system (Equation 1 in Table 2). The way the equations controlling these  
218 three input parameters were established is discussed below.

219

220 Mass normalisation of the measurement signal

221 In most flow analysis methods incorporating a pre-concentration column, the amount of sample loaded is  
222 assumed to remain the same for constant loading times and the resulting peak height signals (expressed  
223 in V) are used for the calculations. Variations in the loaded mass are thus not corrected for. However, this  
224 was found to be an issue as variations in sample mass were observed to be significant during the  
225 "stability experiment", with about 5% decrease in the sample loaded from the first to the last  
226 measurement (data not shown). During the "sample experiment" the average loaded mass for samples  
227 was lower than for the standards, probably due to the fact that the samples were all run at the end of  
228 the sequence and were therefore more likely to be affected by wear on the pump tubing, increased back  
229 pressure on the analytical column and / or changes in the relative flow rates of the sample and buffer  
230 lines (Figure 2). These results show the importance of weighing the amount of seawater loaded each  
231 time and of normalising the peak signal (symbol I, in V) to the loaded mass (in kg). In addition,  
232 gravimetric measurement, coupled with calibration of the analytical balance, provides tighter traceability  
233 to SI (the kg) of the amounts of loaded samples than loading by volumetric means.

234 As a result of this finding, mass normalised signals (symbol J, in  $V\ kg^{-1}$ ) were used throughout this study  
235 for the calculations (Equation 2b, Table 2). Following the example given in Quétel et al. (2001), in  
236 equations 2a, 3a and 4a unity multiplicative factors were introduced to carry standard uncertainties  
237 associated with signal stability, data integration and matrix effects. Since these unity factors do not  
238 influence the final results, but enable the propagation of sources of uncertainty, they are discussed in  
239 more detail below.

240

241 Blank corrections

242 Assessment of overall blank levels that reflect the reality of sample contamination during the  
243 measurement procedure is necessary. In the international inter-laboratory comparison exercise  
244 IRONAGES, blanks were reported to range between 6 and 290% of the Fe content in the seawater  
245 sample (Petrov et al., 2007). Moreover, participants had diverse ways of defining and assessing their  
246 blanks (Bowie et al., 2006) and were, therefore, possibly overlooking different aspects of the  
247 contamination process. Sources of contamination during FI-CL measurements include the Fe present in  
248 reagents (i.e. the added  $H_2O_2$ , the buffer and wash solutions and the chemiluminescence reagents) and  
249 Fe leaching from laboratory ware and parts of the experimental set-up. Sample manipulations could also  
250 be a major contributor to the analytical blank as was shown to be the case by Petrov et al. (2007) during

251 isotope dilution inductively coupled plasma mass spectrometry measurements using co-precipitation with  
252 magnesium hydroxide for sample preparation. The Fe from the reagents of the chemiluminescence  
253 reaction is normally included in the baseline. Baseline subtraction for the determination of net peak  
254 height or peak area signals should therefore remove this possible bias. The influence of additions of  
255 chemical reagents for the purpose of preserving and/or conditioning the samples (e.g. acid, H<sub>2</sub>O<sub>2</sub>) can be  
256 assessed using double spiking of the reagents. Previous studies using FI-CL have shown their contribution  
257 to be low / negligible if care is taken to select high purity reagents (Bowie et al., 2003; Bowie et al.,  
258 2004; Klunder et al. 2010).

259 Descriptions of what a blank may represent are available from the International Union of Pure and  
260 Applied Chemistry (IUPAC). A "procedural blank" is "*where the analytical procedure is executed in all*  
261 *respects apart from the addition of the test portion*" (McNaught and Wilkinson, 1997; Inczedy et al.,  
262 1998). Alternative measurement procedures for blank determination, such as the field blank approach or  
263 varying sample loading times and extrapolating back to time zero (Bowie et al. 2004), were not suitable  
264 as the former requires a matrix containing no analyte and the latter only accounts for reagents that are  
265 loaded for a constant time e.g. the wash solution, but not those for which the amount loaded is variable  
266 e.g. the pH adjustment solution.

267 In FI-CL, the signal obtained with the "closed sample valve" method as described above, i.e. loading only  
268 buffer (Bowie et al., 2004; Ussher et al., 2010a), can be considered as a procedural blank. This method  
269 was applied as no better alternatives could be found for estimating the level of contamination. The risk  
270 that matrix effects and pH changes could influence final results due to fluctuations in the blank values  
271 determined in this way is discussed below. Normalised signal intensities were calculated by division by  
272 the average loaded sample mass (equation 3b). These blank values were 50-100 times lower than the  
273 signals for the seawater samples. Unity multiplicative correction factors were used to propagate  
274 uncertainties on stability and matrix effects (equation 3a) and are discussed in more detail below.  
275

#### 276 Calculation of the calibration slope

277 The FI-CL method has a different sensitivity for seawater than for ultra-pure water because of matrix  
278 related effects (Bucciarelli et al., 2001). Thus, a common approach for the calibration under matrix-  
279 matching conditions is to use a low level Fe seawater and fortify it with increasing amounts of Fe  
280 (Bucciarelli et al., 2001; Bowie et al., 2004; Ussher et al., 2010a; Klunder et al., 2011). In this work, in  
281 addition to the low level seawater alone (termed the 'zero' standard), six calibration standards were  
282 prepared with Fe amount content ranging from 0.15 to 0.9 nmol kg<sup>-1</sup>. Since measurements were  
283 repeated 6 times for each calibration point, a total of 7 x 6 = 42 results were obtained. A linear  
284 regression was plotted, with the masses of Fe loaded (in kg, obtained by multiplication of the standard Fe  
285 mass fraction by the loaded mass of the replicate) on the x axis and the corresponding measured signal

286 intensities (in V) on the y axis. The 'behaviour' of the data was nearly the same irrespective of the scale  
287 of observation, with replicate results spread randomly around the regression graph in more or less the  
288 same way for all 6 standards prepared and tested. Common practice is to produce 3-4 replicates per Fe  
289 level and work with average values. Thus, a more practical way of establishing the calibration curve  
290 consists of plotting a linear regression between the group of 6+1 Fe amount content (C, in nmol kg<sup>-1</sup>) on  
291 the x axis and the corresponding average normalized intensities (J, in V kg<sup>-1</sup>) on the y axis. The sensitivity  
292 coefficient (F, in V nmol<sup>-1</sup>), i.e. the slope, is obtained using equation 4b from Table 2 (see Figure 3).  
293 Weighted regression can also be performed but the calculations are more complex. In a weighted  
294 regression the higher the uncertainty on a y value the smaller the contribution of the y value to the  
295 regression slope. This is especially important if the increase of values on the x axis can be related to an  
296 increase of the standard uncertainty on corresponding values on the y axis. There was no difference with  
297 this dataset at the 95% confidence level between weighted and unweighted regressions. This is probably  
298 because the increase in the standard uncertainty with increased normalised intensity is limited. The  
299 comparison between these two approaches is further discussed in the next section.

300

### 301 ***Assessing the standard uncertainties***

302 Individual uncertainty components and the factors influencing their standard uncertainties were  
303 evaluated. This is necessary to enable a combined uncertainty estimation of the Fe amount content  
304 results.

305

### 306 Uncertainty on mass normalised measurement signals

307 During the "sample experiment", the repeatability (short term signal stability) of mass-normalised  
308 intensities (peak height based signals) for one measurement varied between 1.9 and 4.0% RSD (relative  
309 standard deviation, n=6) while for the "stability experiment" repeatabilities varied between 2.4 and 4.9  
310 %. These variations in RSD cannot be explained by variations in the specific characteristics of the sample  
311 replicates since the same solution was measured throughout the "stability experiment". Moreover, as  
312 illustrated in Figure 4, there was also a longer term variability component involved (within-sequence-  
313 stability), and thus two sources of instability influencing the intensity values. Over the 32 h long analytical  
314 sequence there was no clear trend, and as a result correction for drift was not possible. Therefore, the  
315 approach proposed is to estimate typical values for both components from the outcome of an ANOVA  
316 analysis and multiply the sample average mass normalised intensities by unity correction factors carrying  
317 the uncertainty for these two components ( $\delta_{rep\_S}$  and  $\delta_{stab\_S}$ ). Repeated intensity values per sample and  
318 average intensity values from replicate samples were approximately normally distributed. The intensity  
319 repeatability and the within-sequence-stability, determined using data from the "stability experiment",  
320 were 4.1% and 6.3% respectively. Assuming independence between the intensity values used to

321 calculate both types of standard deviation, uncertainty estimations were carried out using these standard  
322 deviations divided by square root 6, i.e. the number of replicates and square root 5, i.e. the number of  
323 repeat measurements analysed in each case, to give values of 1.7% and 2.8% respectively.

324 Sample loading and standard preparation cannot be performed gravimetrically on board ship and  
325 therefore this is done volumetrically, which may cause additional sources of uncertainty. In this case, the  
326 set of equations described in Table 2 will change slightly and result in equation 6 as described below:

$$327 C_s = \frac{\bar{I}_{R\_S} \cdot \delta_{rep\_S} \cdot \delta_{stab\_S} \cdot \delta_{Wtov\_S} - \bar{I}_{R\_B} \cdot \delta_{stab\_B} \cdot \delta_{rep\_B} \cdot \delta_{matrix\_B}}{F_{reg} \cdot \delta_{matrix\_std}} \quad \text{equation 6}$$

328 As a consequence of not using mass normalization, the sensitivity factor is determined by regression of  
329 the intensity (expressed in V) with the concentration (nmol L<sup>-1</sup>) and has the units V/nmol L<sup>-1</sup>. Secondly,  
330 an extra unity multiplicative correction factor ( $\delta_{Wtov\_S}$ ) was introduced to take account of the difference in  
331 the mass loading between samples and standards (Figure 2). Using this data set and assuming constant  
332 loading (i.e. without mass normalisation) its contribution to the final uncertainty budget was a few  
333 percent. Lastly, although the same approach can be used to quantify the uncertainty on the unity  
334 multiplicative factors of the intensity repeatability and within-sequence-stability, the values will be higher  
335 than in the case of mass normalization. It must be noted that the within-sequence-stability during on-  
336 board measurements might be different than in controlled laboratory conditions, but a specific  
337 assessment was not possible within the time frame of this study.

338 Uncertainty on blank corrections

339 The evaluation of the uncertainty on blank measurement signals was approached in a similar way as for  
340 the sample measurement signals. ANOVA analysis of the "stability experiment" results indicated 6.9%  
341 and 10% respectively for the intensity repeatability (n=5) and the within-sequence-stability. A unity  
342 multiplicative factor  $\delta_{matrix\_B}$  with a value of 1±0.2 was conservatively applied in equation 3a to account  
343 for the matrix differences between the blank samples and the standards used for calibration purposes.  
344 However, since the signal intensity for the analytical blank was about 50-100 lower than the intensity for  
345 the seawater samples in this project, this source of uncertainty on the blank correction had no influence  
346 on the combined uncertainties estimated for the Fe amount content in the samples investigated.

347

348 Uncertainty on the calibration slope

349 As discussed above, there are different statistical approaches that can be used to calculate the slope of  
350 the regression line (Miller, 1991; Press et al., 2012). Values obtained using different regression  
351 approaches are not significantly different at the 95% confident interval, but associated standard

352 uncertainties do vary (Table 3). The standard uncertainty on the slope when using average normalised  
353 intensity values is the same whether the regression is weighted or unweighted. It is lower when using all  
354 individual data in the unweighted regression because there are more data points that follow a normal  
355 distribution. The importance of the number of standards and replicates on the size of the estimated  
356 standard uncertainty of the slope was studied. In Table 4 it can be seen that the number of standards  
357 used is a more important criterion than the number of replicates, but nevertheless the uncertainty on the  
358 sensitivity factor also improves using 6 rather than 3 replicates. Small matrix differences between the  
359 three seawaters tested in the "matrix experiment" did not lead to significant differences between the  
360 slopes obtained for SWA, SWB and SWC. Therefore, no uncertainty factor for differences in the calibrant  
361 matrix was applied.

362

### 363 **Discussion**

#### 364 ***Application to seawater samples from the SAFe and GEOTRACES campaigns***

365 Since consensus values are available for the Fe amount content in samples from the SAFe and  
366 GEOTRACES campaigns (GEOTRACES, 2013), these data were compared with results obtained by  
367 application of the model for combined uncertainty estimation and the calculations described above.  
368 Samples D2, GS and GD were analyzed using 6 replicates each time, the "closed sample valve" approach  
369 for blank assessment and a least square regression calibration line with 7 levels (no Fe added + 6 levels  
370 of added Fe) in SWA. This was the "sample experiment", and results obtained are reported in Table 5.  
371 Estimated expanded (coverage factor  $k=2$ ) relative combined uncertainties were around 12% on a peak  
372 height basis, and around 10% on a peak area basis. Using this dataset, the combined uncertainty was  
373 slightly higher using volumetric loading compared with gravimetric loading. For example, for sample GD  
374 the combined expanded uncertainty increased from 12 to 13% for peak height integration. It can be seen  
375 that both peak height and peak area based results are systematically lower than the consensus values.  
376 Results obtained for GS and GD (peak height and peak area basis) and peak area results for D2 were in  
377 agreement with consensus values within uncertainty statements. These conclusions were reached from  
378 the observation that the expanded combined uncertainty ( $k=2$ ) on the difference between a measured  
379 and the corresponding consensus value was greater than the difference itself in all cases (calculations  
380 according to a methodology reported in Linsinger, 2010). For the peak height results for the D2 sample,  
381 the expanded uncertainty on the difference was smaller than the difference itself but only by less than  
382 3%. These results validate the measurement procedure implemented and the uncertainty estimation  
383 process developed. They nevertheless point to the presence of a systematic effect not yet (sufficiently)  
384 corrected for.

385

386 An overview of the values of the input parameters and their associated standard uncertainties for these  
 387 experiments is given in supplementary Table S1. The relative contributions of the different input  
 388 parameters to the uncertainty budget are given for sample GD in Table 6 as an example. The normalised  
 389 signal intensity repeatability accounts for only 7.9% of the total uncertainty. The within-sequence-stability  
 390 (assessed over 32 h) and the uncertainty on the sensitivity coefficient (calibration slope) are the most  
 391 important contributors to the combined uncertainty with relative contributions of 21.6 and 69.7%.  
 392 Therefore, it is beneficial to have a low uncertainty on the calibration slope. For this reason, it is  
 393 favourable to use sufficient replicates (6) and number of standards (at least the non-spiked standards  
 394 and 5 spiked levels). Moreover, correctly estimating the within-sequence-stability is key and should be  
 395 done under the same measurement conditions as for the samples.  
 396

397 Results obtained indicate that an uncertainty estimation based on the signal repeatability alone, as is  
 398 often done in FI-CL studies, is not a realistic estimation of the overall uncertainty of the procedure.  
 399 However, taking into account only the major contributions, the combined expanded uncertainty could be  
 400 approximated using equation 7:  
 401

$$402 U_{C_s} \approx 2 \cdot C_s \sqrt{\frac{\overline{J}_S^2 \cdot \left[ \left( \frac{u_{\delta_{rep\_S}}}{\delta_{rep\_S}} \right)^2 + \left( \frac{u_{\delta_{stab\_S}}}{\delta_{stab\_S}} \right)^2 \right]}{\left( \overline{J}_S - \overline{J}_B \right)^2} + \left( \frac{u_F}{F} \right)^2} \quad \text{equation 7}$$

403 In this, the standard uncertainty on the intensity repeatability and within-sequence-stability can be  
 404 assessed using ANOVA analyses of repeat measurements of the same solution. The uncertainty on the  
 405 calibration slope can be obtained using statistical tools. This simplified approach assumes that the blank  
 406 does not significantly contribute to the uncertainty and should therefore have a much lower intensity  
 407 compared with the sample (as was the case in this study). When using data from this project the  
 408 uncertainty obtained with equation 7 was nearly identical to the uncertainty calculated above (for  
 409 example the difference was less than 0.2% for GD using peak height data). Therefore, if the assumptions  
 410 are valid this simplified approach provides a realistic uncertainty estimate.  
 412

### 413 ***Peak area versus peak height***

414 The bias between results and consensus values was around -12% for D2 and GS and -20% for GD, on a  
 415 peak height basis, and around -8% for D2 and GS and -16% for GD, on a peak area basis. This also  
 416 means that peak height results were systematically lower than the peak area results by approximately 4-

417 5%. The cause for this trend is not well understood. It is unlikely to be related to an error in the  
418 placement of the baseline for integration, as this affects height less than area (Dyson et al., 1998). In  
419 contrast, the asymmetry of the FI-CL peaks could be a possible source of error during peak height  
420 measurement, since peak area is less sensitive to peak asymmetry than peak height (Dyson et al., 1998).  
421 It can also be observed in Table 5 that estimated combined uncertainties are larger for peak height than  
422 for peak area based results. This is mainly related to a larger uncertainty associated with the sensitivity  
423 coefficient for peak height compared with peak area (Table S1). The intensity repeatability and the  
424 within-sequence-stability are also slightly better for peak area than for peak height data, which can be  
425 related to count statistics. Area integration is considered the 'true' measure of the amount of solute  
426 (Dyson et al., 1998) and possible problems specific to peak area data such as peak overlap and / or low  
427 S/N ratios (Dyson et al., 1998) are not an issue with FI-CL measurements. These observations lead to the  
428 conclusion that peak area data may be preferable to peak height data with FI-CL measurement results,  
429 contrary to common practice. Additionally, users should routinely and systematically describe the way  
430 peak data are processed.

431

### 432 **Comments and recommendations**

433 The amount content of dissolved Fe in marine waters is measured to elucidate the biogeochemical cycling  
434 of this element and its role in the oceanic sequestration of atmospheric CO<sub>2</sub>. However, quantifying the  
435 amount of Fe present in <0.2 µm filtered and acidified seawater samples remains a difficult analytical  
436 task, and achieving reliable results is a challenging objective. Moreover, the uncertainty as part of the  
437 measurement results is easily underestimated.

438 FI-CL is a technique commonly applied because of its portability and hence suitability for shipboard  
439 deployment. This paper proposes that the relative expanded (*k*=2) combined uncertainty of the  
440 measurement results using FI-CL in the described configuration cannot be better than about 10 to 15%  
441 for seawater samples containing 0.5 to 1 nmol kg<sup>-1</sup> of dissolved Fe. When applied on-board ship the  
442 minimum achievable uncertainty is likely to be even larger owing to the more challenging working  
443 conditions compared with shore-based laboratories. Moreover, this paper emphasises the fact that it will  
444 be beneficial to researchers to refine measurement practices in order to improve the likelihood of  
445 achieving lower uncertainty targets. For FI-CL, the uncertainty associated with the calibration slope and  
446 the within-sequence-stability are shown to be much greater sources of uncertainty than the intensity  
447 repeatability alone. Experimental planning must therefore systematically address the identification of  
448 strategies aimed at quantifying and minimising the role of these uncertainty contributors. These  
449 strategies include the use of as many calibration standards as possible (ideally 5 plus the 'zero' standard  
450 measured with 6 replicates) and measurements repeated regularly for the same sample over the entire  
451 analytical sequence. It is also shown that more attention needs to be paid to the way FI-CL peak data are

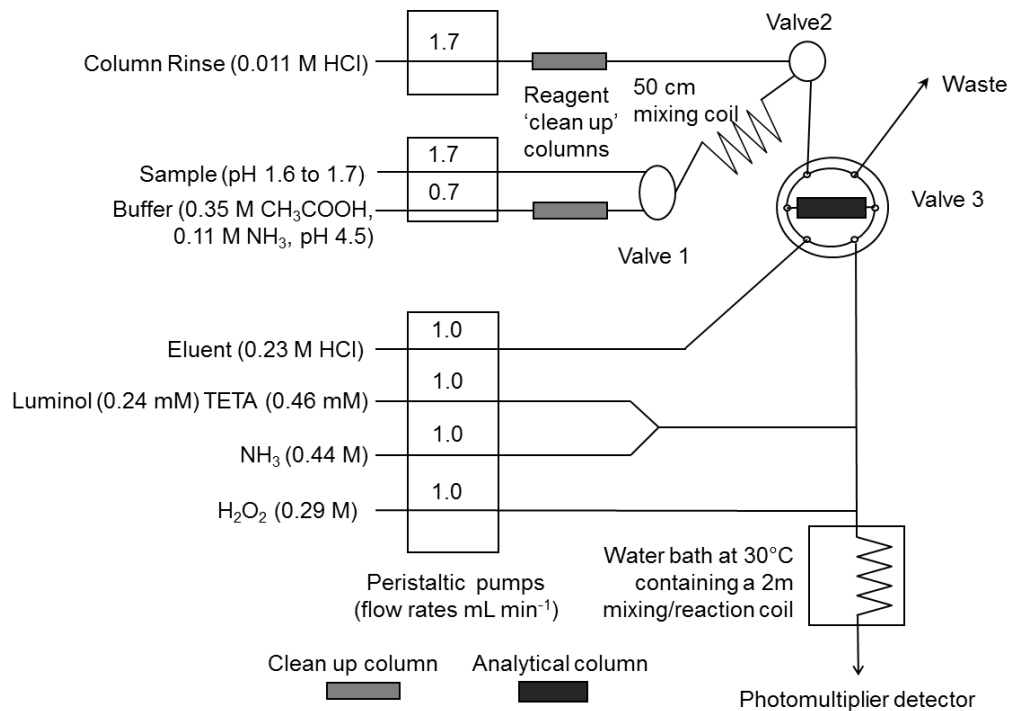
452 collected and processed, as this could lead to significant errors with respect to the size of the combined  
453 uncertainties. To enhance the transparency of these aspects it is recommended that more comprehensive  
454 descriptions of the methods used to validate the measurement procedures (including the way peak data  
455 collection/processing is performed) are included in publications and reports. Moreover, a simple equation  
456 to approximately estimate the uncertainty has been proposed, which is valid if the blank levels are  
457 significantly lower than the levels of interest.

458      **References**

- 459      • Achterberg, E.P., T.W. Holland, A.R. Bowie, R.F.C. Mantoura and P.J. Worsfold, 2001.  
460      Determination of iron in seawater. *Analytica Chimica Acta*, 442: 1-14.
- 461      • Analytical Methods Committee, 1995. Uncertainty of measurement: implications of its use in  
462      analytical science. *Analyst* 120: 2303-2308.
- 463      • Bowie, A.R., E.P. Achterberg, S. Blain, M. Boye, P.L. Croot, P.L., H.J.W. de Baar, P. Laan, G.  
464      Sarthou and P.J. Worsfold, 2003. Shipboard analytical intercomparison of dissolved iron in  
465      surface waters along a north-south transect of the Atlantic Ocean. *Marine Chemistry* 84: 19-34.
- 466      • Bowie, A.R., E.P. Achterberg, P.L. Croot, H.J.W. de Baar, P. Laan, P., J.W. Moffett, S. Ussher and  
467      P.J. Worsfold, 2006. A community-wide intercomparison exercise for the determination of  
468      dissolved iron in seawater. *Marine Chemistry* 98: 81-99.
- 469      • Bowie, A.R., P.N. Sedwick and P.J. Worsfold, 2004. Analytical intercomparison between flow  
470      injection-chemiluminescence and flow injection-spectrophotometry for the determination of  
471      picomolar concentrations of iron in seawater. *Limnology and Oceanography: Methods* 2: 42-54.
- 472      • Boyd, P.W. and M.J. Elwood, 2010. The biogeochemical cycle of iron in the ocean. *Nature Geoscience* 3: 675-682.
- 473      • Bucciarelli, E., S. Blain and P. Tréguer, 2001. Iron and manganese in the wake of the Kerguelen  
474      Islands (Southern Ocean). *Marine Chemistry* 73: 21-36.
- 475      • Dyson, N., 1998. Chapter 2: Errors in peak area measurement. In *Chromatographic Integration  
476      Methods*. The Royal Society of Chemistry. pp. 35-88.
- 477      • GEOTRACES, 2013. Dissolved Iron – values in nmol/kg Consensus values ( $\pm$  1 std. dev.) for SAFe  
478      Reference Samples as of May 2013. [http://www.geotrades.org/science/intercalibration/322-  
479      standards-and-reference-materials](http://www.geotrades.org/science/intercalibration/322-standards-and-reference-materials) (last accessed July 15, 2014)
- 480      • Gledhill, M.B, and K.N. Buck, 2012. The organic complexation of iron in the marine environment:  
481      A review. *Frontiers in microbiology* 3: 1-17.
- 482      • Inczedy, J., T. Lengyel, A. Ure, A. Gelencsér and A. Hulanicki, 1998. *Compendium of analytical  
483      nomenclature*. Blackwell Science Ltd., Oxford, UK.
- 484      • ISO/IEC, General requirements for the competence of testing and calibration laboratories,  
485      ISO/IEC 17025:2005, International Organization for Standardization/International Electrotechnical  
486      Commission, Geneva, 2005.
- 487      • JCGM 100, Evaluation of measurement data — Guide to the expression of uncertainty in  
488      measurement; Joint Committee for Guides in Metrology (BIPM, IEC, IFCC, ISO, IUPAC, IUPAP,  
489      OIML, ILAC), BIPM, [www.bipm.org](http://www.bipm.org), Paris, 2008.
- 490

- 491 • JCGM 200, International vocabulary of metrology — Basic and general concepts and associated  
492 terms (VIM); Joint Committee for Guides in Metrology (BIPM, IEC, IFCC, ISO, IUPAC, IUPAP,  
493 OIML, ILAC), BIPM, [www.bipm.org](http://www.bipm.org), Paris, 2008
- 494 • Johnson, K. S., E.Boyle, K. Bruland, K. Coale, C. Measures, J. Moffett, A. Aguilar-Islas, K.  
495 Barbeau, B. Bergquist, A. Bowie, K. Buck, Y. Cai, Z. Chase, J. Cullen, T. Doi, V. Elrod, S.  
496 Fitzwater, M. Gordon, A. King, P. Laan, L. Laglera-Baquer, W. Landing, Lohan, J. Mendez, A.  
497 Milne, H. Obata, L. Ossiander, J. Plant, G. Sarthou, P. Sedwick, G. J. Smith, B. Sohst, S. Tanner,  
498 S. Van den Berg and J. Wu, 2007. Developing standards for dissolved iron in seawater. *Eos, Transactions of the American Geophysical Union* 88: 131-132.
- 500 • Klunder, M., P. Laan, R. Middag, H. de Baar and J. Van Ooijen, 2011. Dissolved iron in the  
501 Southern Ocean (Atlantic sector). *Deep Sea Research Part II: Topical Studies in Oceanography*  
502 58: 2678-2694.
- 503 • Linsinger, T., 2010. Comparison of a measurement result with the certified value. European  
504 Reference Materials: Application Note 1.
- 505 • Lohan, M.C., A.M. Aguilar-Islas and K.W. Bruland, 2006. Direct determination of iron in acidified  
506 (pH 1.7) seawater samples by flow injection analysis with catalytic spectrophotometric detection:  
507 Application and intercomparison. *Limnology and Oceanography: Methods* 4: 164-171.
- 508 • Martin, J. and S. Fitzwater, 1988. Iron deficiency limits phytoplankton growth in the north-east  
509 Pacific subarctic. *Nature* 331: 341-343.
- 510 • Mawji, E., M. Gledhill, J.A. Milton, G.A. Tarhan, S. Ussher, A. Thompson, G.A. Wolff, P.J.  
511 Worsfold, and E.P. Achterberg, 2008. Hydroxamate siderophores: Occurrence and importance in  
512 the Atlantic Ocean. *Environmental Science & Technology* 42: 8675-8680.
- 513 • McNaught, A.D. and A. Wilkinson, 1997. Compendium of chemical terminology, Blackwell Science  
514 Oxford.
- 515 • Metrodata GmbH, 2003. Gum Workbench. The software tool for the expression of uncertainty in  
516 measurement. Metrodata GmbH, D-79639 Grenzach-Wyhlen, Germany.
- 517 • Miller, J.N., 1991. Basic statistical methods for analytical chemistry. Part 2. Calibration and  
518 regression methods. A review. *Analyst* 116: 3-14.
- 519 • Mills, M.M., C. Ridame, M. Davey, J. La Roche and R.J. Geider, (2004) Iron and phosphorus co-  
520 limit nitrogen fixation in the eastern tropical North Atlantic. *Nature* 429: 292-294.
- 521 • Nordic Committee on Food Analysis (NMKL), 1997. Pathogenic Vibrio species. Detection and  
522 enumeration in foods. Method n°156 (UDC 576.851)
- 523 • Obata, H., H. Karatani and E. Nakayama, (1993) Automated determination of iron in seawater by  
524 chelating resin concentration and chemiluminescence detection. *Analytical Chemistry* 65: 1524-  
525 1528.

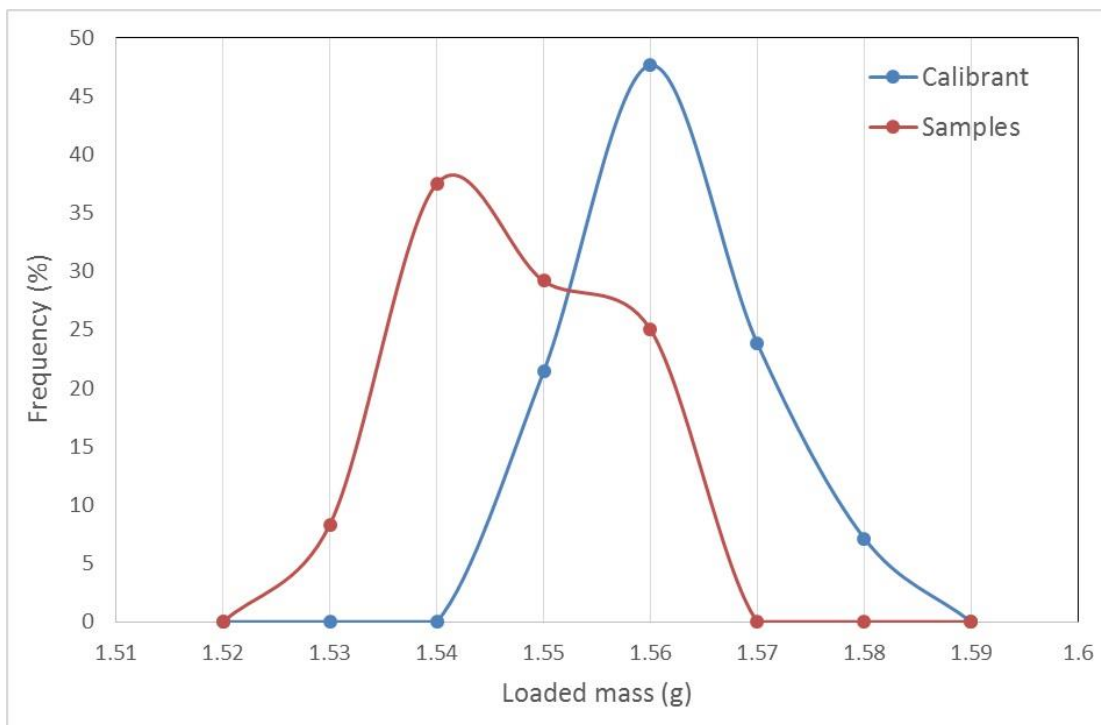
- 526 • Petrov, I., C.R. Quétel and P.D.P. Taylor, (2007) Investigation on sources of contamination, for  
527 an accurate analytical blank estimation, during measurements of the Fe content in seawater by  
528 isotope dilution inductively coupled plasma mass spectrometry. *Journal of Analytical Atomic*  
529 *Spectrometry* 22, 608-615.
- 530 • Press, W.H., 2012. *Numerical Recipes in C: The Art of Scientific Computing*.
- 531 • Quétel, C.R., T. Prohaska, S.M. Nelms, J. Diemer and P.D.P. Taylor, 2001. ICP-MS applied to  
532 isotope abundance ratio measurements: performance study and development of a method for  
533 combining uncertainty contributions from measurement correction factors. In: G. Holland and S.  
534 Tanner (Editors), *Plasma Source Mass Spectrometry: The New Millennium*. 7th Durham  
535 Conference Royal Society of Chemistry, Cambridge, pp. 257
- 536 • Ussher, S.J., E.P. Achterberg, C. Powell, A.R. Baker, T.D. Jickells, R. Torres and P.J. Worsfold,  
537 2013. Impact of atmospheric deposition on the contrasting iron biogeochemistry of the North and  
538 South Atlantic Ocean. *Global Biogeochemical Cycles* 27: 1-12.
- 539 • Ussher, S.J., E.P. Achterberg, G. Sarthou, P. Laan, H.J.W. de Baar and P.J. Worsfold, 2010a.  
540 Distribution of size fractionated dissolved iron in the Canary Basin. *Marine Environmental*  
541 *Research* 70: 46-55.
- 542 • Ussher, S.J., E.P. Achterberg and P.J. Worsfold, 2004. Marine Biogeochemistry of Iron.  
543 *Environmental Chemistry* 1: 67-80.
- 544 • Ussher, S.J., I. Petrov, C.R. Quétel and P.J. Worsfold, 2010b. Validation of a portable flow  
545 injection-chemiluminescence (FI-CL) method for the determination of dissolved iron in Atlantic  
546 open ocean and shelf waters by comparison with isotope dilution-inductively coupled plasma  
547 mass spectrometry (ID-ICPMS). *Environmental Chemistry* 7: 139-145.
- 548 • Wu, J.F., E. Boyle, W. Sunda and L.S. Wen, 2001. Soluble and colloidal iron in the oligotrophic  
549 North Atlantic and North Pacific. *Science* 293: 847-849.
- 550 • Wyatt, N.J., A. Milne, E.M.S. Woodward, A.P. Rees, T.J. Browning, H.A. Bouman, P.J. Worsfold  
551 and M.C. Lohan, 2014. Biogeochemical cycling of dissolved zinc along the GEOTRACES South  
552 Atlantic transect GA10 at 40°S. *Global Biogeochemical Cycles* 10.1002/2013GB004637.



554

555 **Figure 1: The FI-CL system used for the determination of dissolved Fe levels in seawater.**

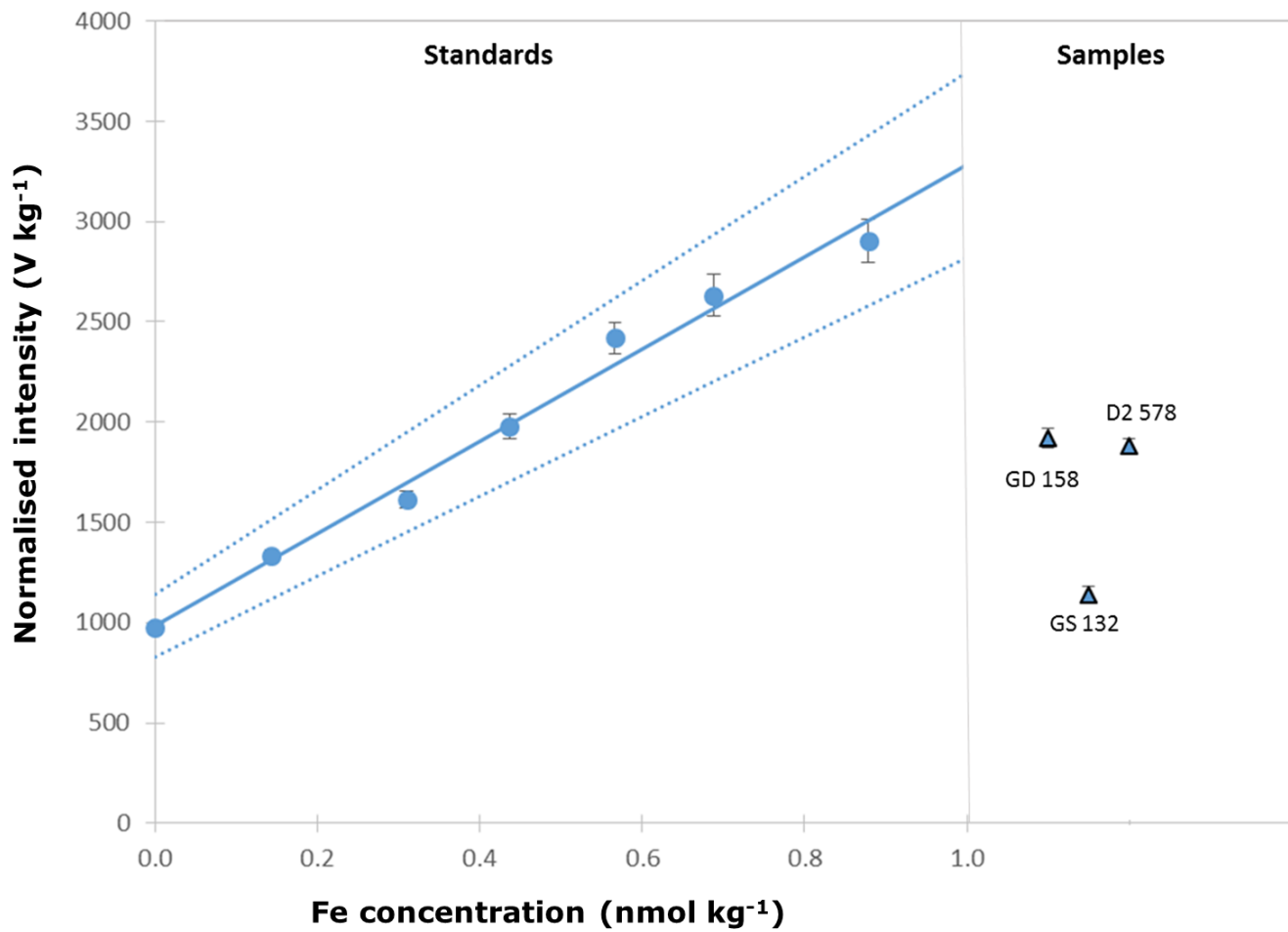
556



557

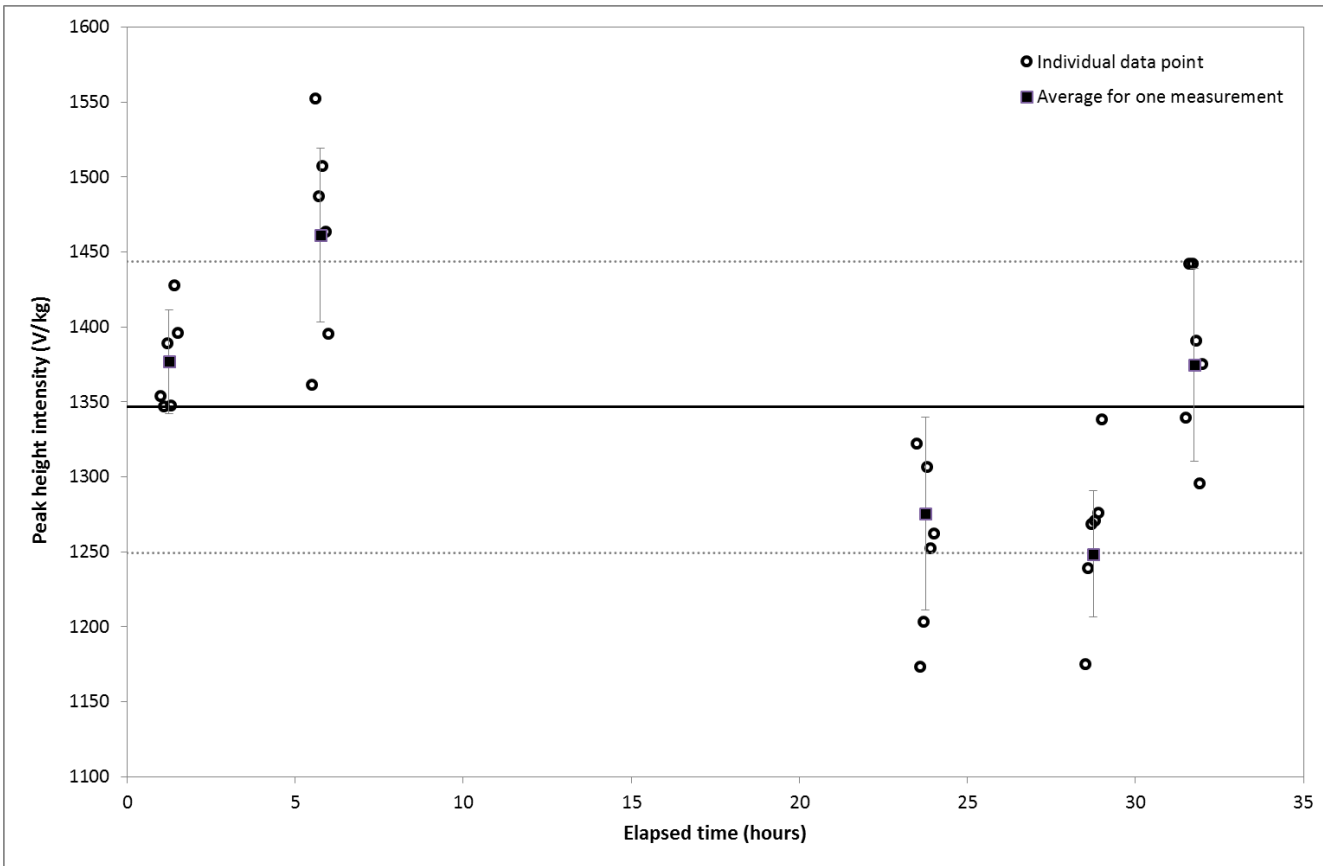
558 **Figure 2: Frequency of variation (in %) of loaded masses for samples and calibration standards  
559 during the “sample experiment”**

560



561  
562  
563  
564  
565  
566  
567

Figure 3: Unweighted calibration using average data for the regression. Blue dotted lines delimit a 95% confidence interval around the regression graph. Signal intensities observed for samples GD158, GS132 and D2578 are also reported.



570 **Table 1: Description of the samples used.**

<b>Sample name</b>	<b>SWA</b>	<b>SWB</b>	<b>SWC</b>	<b>SAFe campaign</b>	<b>GEOTRACES campaigns</b>	
				<b>D2-578</b>	<b>GS-132</b>	<b>GD-158</b>
Collection Location	05°20.5' S, 06°11.9' W to 06°44.8' S, 05°04.8 W	27° 47.195' S, 007°1 2.949' W	40° S 48.46° W	30° N, 140° W	31°40' N 64°10' W	31°40' N 64°10' W
Depth	Surface	500 m	Surface	1000 m	Surface	2000 m
Filtration	Sartorius Sartobran-P cartridge. Cellulose acetate 0.45 µm pre-filter then 0.2 µm filter	Whatman GD/X PTFE 0.2 µm filter	Pall Acropak Supor capsule. PES 0.8 pre-filter then 0.2 µm filter.	Polycarbonate track etched 0.45 µm pre-filter, then 0.2-µm filter. Homogenized in 1000 L fluorinated LDPE tanks	Pall Acropak Supor capsule. PES0.8 pre-filter then 0.2 µm filter.	
Acidification	Bulk sample acidified at sea with 700 mL of ~10 M Q-HCl. Homogenized in 1000 L fluorinated LDPE tanks	Acidified at Plymouth University (PU) with 2 mL of Romil UpA grade HCl per L seawater	Acidified at PU with 1 mL of Romil UpA grade HCl per L seawater	Acidified at sea with 2 mL of conc HCl per L seawater.	Homogenized in 500 L fluorinated LDPE tanks. Acidified at sea with 2 mL of conc HCl.	
Final pH	2.0	2.0	1.7	1.8	1.8	1.8
Consensus dissolved Fe ± 2 s.d. (nmol kg⁻¹)	0.53 ± 0.20	N/A	N/A	0.933 ± 0.046	0.546 ± 0.092	1.0 ± 0.2
Reference	Bowie et al., 2006	Ussher et al., 2013	Wyatt et al., 2014	Lohan et al., 2006	Johnson et al, 2007	

571

**Table 2: Mathematical equations for quantification of the Fe amount content using gravimetric loading and FI-CL based procedure.**

<b>1. Amount content in the sample <math>C_S</math></b>
Blank corrected sample signal intensity divided by the sensitivity (calibration slope) of the measurement procedure :
$C_S = \frac{\bar{J}_S - \bar{J}_B}{F}$
<b>2. Normalised signal intensity for the sample <math>\bar{J}_S</math></b>
a. Normalised signal intensity for the sample accounting for all sources of uncertainty: $\bar{J}_S = \bar{J}_{R\_S} \cdot \delta_{rep\_S} \cdot \delta_{stab\_S}$
b. Average normalised raw signal intensity for consecutive replicates: $\bar{J}_{R\_S} = \frac{1}{n} \sum_i \frac{I_{S\_i}}{m_{S\_i}}$
<b>3. Normalised signal intensity for the analytical blank <math>\bar{J}_B</math></b>
a. Normalised signal intensity for the analytical blank accounting for all sources of uncertainty: $\bar{J}_B = \bar{J}_{R\_B} \cdot \delta_{stab\_B} \cdot \delta_{rep\_B} \cdot \delta_{matrix\_B}$
b. Average normalised raw signal intensity for consecutive replicates under closed sample valve conditions: $\bar{J}_{R\_B} = \frac{1}{n} \sum_i \frac{I_{B\_i}}{\bar{m}_S}$
<b>4. Calibration slope F</b>
a. Slope accounting for all sources of uncertainty: $F = F_{reg} \cdot \delta_{matrix\_std}$
b. Slope of least squares regression line of the normalised signal intensity versus the amount added Fe:
$F_{reg} = \frac{r \sum C_{std\_j} \cdot \bar{J}_{std\_j} - \sum C_{std\_j} \cdot \sum \bar{J}_{std\_j}}{r \sum C_{std\_j}^2 - (\sum C_{std\_j})^2}$
<b>5. Amount content of the added Fe in the calibration standards</b>
a. Added Fe amount in the calibration standard: $C_{std\_j} = \frac{m_{stock\_j}}{(m_{stock\_j} + m_{calSW\_j})} \cdot C_{stock}$
b. Amount in the stock solution: $C_{stock} = \frac{m_{mother\_aliquot}}{m_{stock} + m_{mother\_aliquot}} \cdot C_{mother}$

Parameter		Index	
C	Fe amount content (nmol kg <sup>-1</sup> )	S	Sample
I	Signal intensity (V)	B	Blank
$\bar{J}$	Average mass normalised intensity (V kg <sup>-1</sup> )	R	Raw
		Std	Calibration Standard
F	Sensitivity coefficient (slope, V nmol <sup>-1</sup> )	stock	Intermediate Fe standard stock solution (prepared dilution of the mother solution)
n	Number of replicates	mother	Mother Fe standard solution (commercial standard)
r	Number of calibration standards	i	Index referring to the x <sup>th</sup> sample replicate
m & $\bar{m}$	Mass & average mass (kg)	j	Index referring to the x <sup>th</sup> standard
		Reg	Sensitivity coefficient (calibration slope) obtained by linear regression
		calSW	a 'low iron' seawater substrate used to produce the calibration curves
$\delta$	Unity multiplicative correction factors carrying the relative uncertainty associated to the parameter considered	Stab	Accounts for the uncertainty arising from the intensity stability over an analytical sequence
		matrix	Accounts for the uncertainty arising from matrix effects on the sensitivity
		rep	Accounts for the uncertainty arising from the intensity repeatability
		WtoV	Accounts for the uncertainty related to the difference in loaded mass whether it is done by weighing or volumetrically

577      **Table 3: Slopes and their associated standard uncertainties depending on the regression calculations**  
 578      **considered. r is the number of standards and n the number of replicates per standard.**

Regression approach		Data points	Sensitivity coefficient (=slope) (F)	
			Value	Uncertainty (k=1)
Weighted regression		7 (r)	2301	83
			2297	118
			42 (r*n)	56

579

580      **Table 4: Dependence of the relative standard uncertainty (rsu) on the calculated slope/sensitivity coefficient,**  
 581      **rsu (F), in %, on the number of replicates or calibration standards used.**

n	rsu (F), with n = number of replicates using 7 calibration standards (original + 6 Fe addition levels)	rsu (F), with n = number of calibration standards using 6 replicates for each standard
6	6.6	6.6
5	7.5	6.8
4	7.9	11.5
3	8.6	14.6

582

583      **Table 5: Amount content results with combined expanded uncertainty with a coverage factor (k) of 2 (i.e. 95% confidence interval) for the three sea water samples from the SAFe and GEOTRACES campaigns using gravimetric loading. Consensus values were downloaded from the GEOTRACES.org website and are from May 584      2013.**

Sample	Obtained Fe amount content (nmol kg <sup>-1</sup> )				Consensus Fe amount content (nmol kg <sup>-1</sup> )	
	Peak height		Peak area			
	Value	Relative uncertainty	Value	Relative uncertainty	Value	Relative uncertainty
D2	0.82 ± 0.10	12	0.861 ± 0.086	10	0.933 ± 0.046	4.9
GS	0.478 ± 0.060	12	0.500 ± 0.051	10	0.546 ± 0.092	16.8
GD	0.800 ± 0.099	12	0.836 ± 0.084	10	1.0 ± 0.2	20.0

587

588

589

590

591

592

593

594

595  
 596 **Table 6: Relative contributions (%) to the combined uncertainty budget estimated for the dissolved Fe level**  
 597 **measured by FI-CL in the GD sample from the GEOTRACES campaign (symbols as in Table 2). The intermediate**  
**result refers to the parameters used in equation 1 of Table 2, in which all associated uncertainties are included.**

Quantity		Gravimetric loading	
		Peak height	Peak area
$\bar{J}_S$ (V/kg)	<b>Intermediate result</b>	<b>29.5</b>	<b>44.4</b>
	$\bar{J}_{R\_S}$ (treated as constant)	-	-
	$\delta_{rep\_S}$	7.9	9.4
	$\delta_{stab\_S}$	21.6	35.0
$\bar{J}_B$ (V/kg)	<b>Intermediate result</b>	<b>0.6</b>	<b>1.4</b>
	$I_B$ (treated as constant)	-	-
	$\bar{m}_S$	0.0	0.0
	$\delta_{rep\_B}$	0.0	0.6
	$\delta_{stab\_B}$	0.1	0.0
	$\delta_{matrix\_B}$	0.5	0.8
F (sensitivity coefficient or slope) (V/nanomol)	<b>Intermediate result</b>	<b>69.7</b>	<b>54.3</b>
	$F_{reg}$	69.7	54.3
	$\delta_{matrix\_std}$	0.0	0.0

598

599

600    **Supplementary information**

601    Table S1: details of the uncertainty budget associated to the result of the measurement by FI-CL (with gravimetric loading) of the dissolved Fe amount  
 602    content in the D2 reference material from SAFe. Symbols as in Table 2.

603

Quantity	Intermediate result		Peak height			Peak area		
			Value	Stand Unc (k=1)		Value	Stand Unc (k=1)	
				Absolute	%		Absolute	%
$\bar{J}_S$ (V/kg)	D2	<b>1918</b>	<b>63</b>	<b>3.3</b>		<b>52179</b>	<b>1700</b>	<b>3.3</b>
		<b>GS</b>	<b>1140</b>	<b>37</b>	<b>3.3</b>	<b>30809</b>	<b>1000</b>	<b>3.3</b>
		<b>GD</b>	<b>1879</b>	<b>62</b>	<b>3.3</b>	<b>50711</b>	<b>1700</b>	<b>3.3</b>
	$\bar{J}_{R\_S}$	D2	1918	0	0	52179	0	0
		GS	1140	0	0	30809	0	0
		GD	1879	0	0	50711	0	0
	$\delta_{rep\_S}$		1	0.017	1.7	1	0.015	1.5
	$\delta_{stab\_S}$		1	0.028	2.8	1	0.029	2.9
	<b>Intermediate result</b>		<b>41.8</b>	<b>2.2</b>	<b>5.3</b>	<b>1115</b>	<b>190</b>	<b>17.0</b>
$\bar{J}_B$ (V/kg)	$I_B$		0.0645	0	0	1.72	0	0.0
	$\bar{m}_S$		0.001542	0.000004	0.3	0.001542	0.000004	0.3
	$\delta_{rep\_B}$		1	0.069	6.9	1	0.17	17.0
	$\delta_{stab\_B}$		1	0.10	10	1	0	0
	$\delta_{matrix\_B}$		1	0.2	20	1	0.2	20
	<b>Intermediate result</b>		<b>2297</b>	<b>118</b>	<b>5.1</b>	<b>59330</b>	<b>2190</b>	<b>3.7</b>
F (sensitivity coefficient or slope) (V/nanomol)	$F_{reg}$		2297	118	5.1	59330	2190	3.7
	$\delta_{matrix\_std}$		1	0	0	1	0	0

604